Turkish Journal of Electrical Engineering & Computer Sciences

http://journals.tubitak.gov.tr/elektrik/

Research Article

Turk J Elec Eng & Comp Sci
(2014) 22: 465 – 478
© TÜBİTAK
doi:10.3906/elk-1207-132

Feature selection on single-lead ECG for obstructive sleep apnea diagnosis

Hüseyin GÜRÜLER[1,2,*], **Mesut ŞAHİN**[2], **Abdullah FERİKOĞLU**[3]
[1]Department of Information Systems Engineering, Faculty of Technology,
Muğla Sıtkı Koçman University, Muğla, Turkey
[2]Department of Biomedical Engineering, New Jersey Institute of Technology, Newark, New Jersey, USA
[3]Department of Electrical & Electronics Engineering, Faculty of Engineering, Sakarya University, Sakarya, Turkey

Received: 01.08.2012 • **Accepted:** 25.09.2012 • **Published Online:** 17.01.2014 • **Printed:** 14.02.2014

Abstract: Many articles that appeared in the literature agreed upon the feasibility of diagnosing obstructive sleep apnea (OSA) with a single-lead electrocardiogram. Although high accuracies have been achieved in detection of apneic episodes and classification into apnea/hypopnea, there has not been a consensus on the best method of selecting the feature parameters. This study presents a classification scheme for OSA using common features belonging to the time domain, frequency domain, and nonlinear calculations of heart rate variability analysis, and then proposes a method of feature selection based on correlation matrices (CMs). The results show that the CMs can be utilized in minimizing the feature sets used for any type of diagnosis.

Key words: Heart rate variability, sleep apnea, feature selection, correlation matrices, diagnosing, classification

1. Introduction

Electrocardiograms (ECGs) contain vital characteristics that can help in the detection of abnormalities of the heart. The ECG period, which typically has 5 deflections, P-QRS-T, arbitrarily named 'P' to 'T' waves with the Q, R, and S waves occurring in rapid succession, varies in each cycle. That is, the shape, size, and intervals of the P-QRS-T components are slightly different. Therefore, the heart rate (HR) varies continuously during the day in healthy people. Some disease conditions, like epilepsy and anorexia nervosa, modulate this variation, as well. With this perspective, various characteristic features based on the spread and pattern of ECG have been extracted and used for diagnostic purposes.

The HR increases with sympathetic activity and decreases with parasympathetic activity. The balance between these 2 alternately moving parts of the autonomic nervous system (ANS) is defined as the sympathovagal balance (SB) and is thought to be manifested in the rhythmic changes of the cardiac system [1]. The sympathetic mode influences the low frequency (LF), while both the sympathetic and parasympathetic modes affect the high frequency (HF). Thus, spectral analysis is typically used to estimate SB by looking at the LF and the HF bands of the interbeat (RR) intervals (beat-to-beat intervals, where R is a point corresponding to the peak of the QRS complex of the ECG wave and RR is the interval between successive Rs). The LF/HF ratio bands are employed to assess the SB [2].

Obstructive sleep apnea (OSA) is a serious sleep disorder caused by intermittent episodes of partial or complete obstruction of the upper airway [3,4]. OSA perturbs the cardiac and neuronal activities and disrupts

*Correspondence: hguruler@mu.edu.tr

the sleep pattern, which can be detected via ECG and electroencephalogram (EEG) recordings. OSA is usually diagnosed in a polysomnography (PSG) session conducted in a sleep laboratory [5]. PSG is utilized to determine physiological sleep and its various stages and sleep disorders, such as insomnia, OSA, restless legs syndrome, and periodic leg movement disorders. However, PSG testing is expensive and it requires the connection of various sensors and electrodes (e.g., EEG, electrooculogram, electromyogram, and ECG) to the subject [6].

As discussed by de Chazal et al. [7], automated diagnosis systems are important in that they provide simplicity for the diagnosis of OSA. There are several types of OSA detection methods in the literature that are based on ECG signals [8], some of which also include the respiratory signal [9], EEG [10], blood oxygen saturation (SaO_2) [11], and acoustic properties of the snore sounds [12].

If OSA could be diagnosed with ECGs alone, the sleep session would be much easier to conduct, convenient for the subject, and inexpensive [13]. QRS-based features are useful for apnea identification [14,15]. However, the extraction of ECG characteristics using heart rate variability (HRV) is an advantageous method to study [16,17]. The HRV is the continuous changes in the RR intervals. HRV analysis is a popular noninvasive tool for detecting ANS function [18]. The detection of OSA can be performed and significantly improved through the HRV analysis, since fluctuations in the SaO_2 value of the blood, accompanied by apneic episodes, cause variations in the HR [19,20]. The SB was used as a criterion for the detection of OSA in many studies [13,21].

Although high accuracies of OSA detection and significant successes in apnea classification can be achieved, it is still unclear which feature parameters are more effective. One review [13] presented a systematic comparison of studies that detected OSA based on the same ECG recordings with different algorithms. HRV with or without respiratory signals is analyzed for OSA diagnosis in 3 main categories in general: time, frequency, and nonlinear analysis. Each analysis technique produces a set of features that are mostly numerical. These values are used in decision-making algorithms or mathematical models that may involve neural networks (NNs), support vector machines, wavelets, etc. Thus far, many combinations of time, frequency, and nonlinear domain features of the HRV obtained by ECG have been tested with different types of classification methods. Additionally, some studies report obstructive apneic epoch classification using single-lead ECG. The Apnea-ECG database in PhysioBank was used in this study due to its availability and the opportunity to compare our results with other works based on the same database.

This study aims to classify precollected sleep data into 1 of the 3 basic types: apnea, hypopnea, and healthy episodes, with fewer parameters obtained from single-lead ECG recordings. This article is based on a combination of time-frequency domain functions and nonlinear techniques in the HRV analysis. The contribution of this study, which is compared to the earlier reports where it offers a new feature selection method, presents the most effective features to optimize classifiers.

2. Materials and methods

This study is aimed at classifying OSA in 1 of the 3 basic classes: apnea, hypopnea, and healthy episodes. Figure 1 describes the steps of this classification process.

First, R points and then RR intervals are detected for each ECG recording. Before the HRV analysis, the RR signal correction takes place to eliminate errors, which might still be present in the RR interval series, such as ectopic beats, artifacts, and outliers. If any RR interval is shifted from a previous RR interval by more than 0.3 ms, it is assumed to be erratic and is then replaced by the average of its previous and the next RR intervals. Feature extraction is realized by the time, frequency, and nonlinear techniques detailed below. The HRV analysis involves the previous 3 steps and provides a number of parameters having various degrees

of importance for classification. Correlation matrices (CMs) are formed to select the parameters, which are preferred as inputs to the neural networks. The CMs find the correlation coefficients (CCs) for every single column in relation to the target column. A higher correlation implies a better classification ability for the NNs. The feed-forward backpropagation NN (FBPNN) is utilized in the classification process of this study.

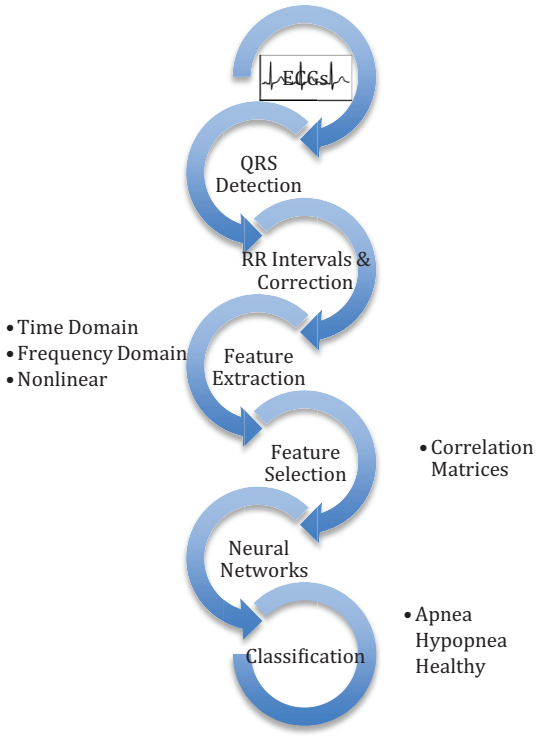

Figure 1. The classification process.

2.1. OSA dataset

The classification of OSA is realized on the Apnea-ECG database in PhysioBank [22]. PhysioBank is a large and growing archive of well-characterized digital recordings of physiological signals and related data for use by the biomedical research community. Table 1 gives the demographic and clinical features of the dataset.

Table 1. Features of the dataset.

	All subjects	Apnea	Hypopnea	Healthy	P-value
Subjects (n)	70	40	10	20	-
Age (years)	45.6 ± 10.6	51.5 ± 7.6	47.2 ± 5.9	32.9 ± 5.4	NS
Males (n)	57	38	8	11	$P < 0.01$
BMI (kg/m^2)	28.1 ± 6.5	30.8 ± 4.6	30.4 ± 9.2	21.3 ± 1.9	NS
Records (h)	8.2 ± 0.5	8.4 ± 0.4	8.0 ± 0.6	7.9 ± 0.4	NS
AHI (e/h)	-	45.4 ± 22.5	12.1 ± 12.0	0.0 ± 0.0	$P < 0.01$

The form of data is mean ± SD or n; BMI: body mass index; AHI: apnea-hypopnea index; NS: no significant statistical difference. Depending on the AHI, recordings containing apneic periods of 100 min or more are classified as apnea, between 5 and 99 min as hypopnea, and fewer than 5 min as healthy.

The data consist of 70 records, divided equally into learning and test sets. Each dataset includes a digitized ECG signal from an uninterrupted recording episode (16 bits/sample, 100 samples/s, and 200 A/D units/mV). The lengths of the recordings vary from 7 to 10 h. The learning and test recordings belong to 1 of the 3 classes, namely apnea, hypopnea, and healthy episodes, depending on the apnea-hypopnea index (AHI) [23].

2.2. Software toolbox

The WaveForm Database (WFDB) is specially designed software for the viewing and analyzing of PhysioBank data. We utilized this software to generate binary annotation files in order to detect QRS intervals from ECG files. QRS was detected for all of the recordings using 'sqrs125', which is a single-lead QRS detector and one of the library functions in the WFDB. The 'ann2rr' is another library function used to get a pick time of each QRS from annotation files.

'Kubios HRV' is an advanced tool for HRV analysis that includes commonly used time-domain (TD) and frequency-domain (FD) HRV parameters [24]. Moreover, Kubios HRV includes a wide variety of different analysis options of the HRV, it is easy to adapt to PhysioBank sources, and presents the analysis results with graphical representations along with the desired file format. Therefore, the software is found to be suitable for this study. The FD involves Fourier transform- and autoregressive modeling-based spectrum analyses. Additionally, some nonlinear HRV analyses are utilized, such as Poincaré and recurrence plots, and approximate and sample entropies. The MATLAB NN toolbox is used for classification.

2.3. Analysis methods

The present study utilizes a variety of significant and relevant characteristic features that include the morphological information, duration, and complexity details of the ECG to classify OSA patient states. The feature sets obtained from the analysis methods are the TD, FD, and nonlinear methods. All of the presented HRV measures are mainly based on the guidance of [25] and are summarized with their formulas in the Appendix of this paper.

2.3.1. Time-domain methods

The TD methods are applied directly to the series of successive RR intervals to reflect the short- and long-term variations. The TD measures include the mean and standard deviation (SD) value of the RR intervals ($\bar{RR}$, SDNN), the mean and SD of the HR ($\bar{HR}$, SDHR), the root-mean-square value of successive differences (RMSSD), and the number of successive intervals of more or less than 50 ms (NN50) and its percentage (pNN50). Geometric measures such as the HRV triangular index and the baseline width of the RR histograms (TINN) are also calculated and added to the analysis.

2.3.2. Frequency-domain methods

The FD analysis is performed using fast Fourier transform (FFT) and autoregressive (AR) modeling. The advantage of FFT-based methods is the simplicity of implementation, while the AR spectrum yields improved resolution, especially for short samples. In HRV analysis, the power spectrum density estimation is carried out using the FFT-based Welch's periodogram method and parametric AR modeling-based methods. As a general approach, the frequency bands of the HRV recordings belonging to very low frequency (VLF), LF, and HF are preferred at 0–0.04 Hz, 0.04–0.15 Hz, and 0.15–0.4 Hz, respectively. The FD measures involve the absolute and

relative powers of the above-mentioned bands and their peak frequencies, along with the LF/HF ratio. The band powers are gained from the absolute values by means of the ratio of its power to the total power. When normalized units are calculated, like LF(n.u.), the VLF power is removed from the total power.

2.3.3. Nonlinear methods

The nonlinear methods that are used in this study are Poincaré plot [26,27], approximate entropy (ApEn) [28], sample entropy (SampEn) [29], detrended fluctuation analysis (DFA) [30], correlation dimension (CD) [31], and recurrence plot (RP) [32]. Each nonlinear analysis investigates the signals from different directions, e.g., complexity, irregularity, or short- or long-term variability.

Poincaré plots are quite definitive and hold essential features that represent the correlation between successive RRs, as illustrated in Figure 2.

Therein, SD1 explains the short-term variation that is principally effected by respiratory sinus arrhythmia, which is the most obvious periodic component of HRV, and it is related to the TD measure, SDSD. On the other hand, SD2 describes the long-term variability that is related to TD measures, SDNN, and SDSD [26].

ApEn is generally used for calculating the complexity or irregularity of the signal [29]. SampEn is similar to ApEn. However, SampEn was formed to decrease the bias of ApEn [33]. The DF analysis is employed to obtain the correlations, which are basically split into short- and long-term changes, throughout the signal [34] (see Figure 3).

The CD measures the complexity of the RR intervals and provides information on the lowest possible dynamic variables. The CD was proposed in [35]. Another method that is also used for analyzing the complexity of the RR intervals is RP [32]. The quantitative measures of RPs included in this study are the recurrence rate (REC), which is simply the ratio of ones and zeros in the RP matrix; Lmean is the average diagonal line length; DET is the determinant of the RR intervals as measured by the variable; and Shannon entropy (ShanEn) is the line length distribution.

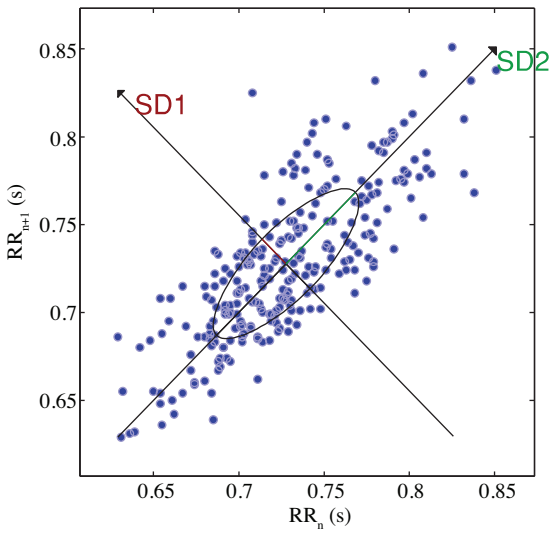

Figure 2. Poincare plots. SD1 and SD2 are the SDs in the directions x_1 and x_2, where x_2 is the line-of-identity for which $RR_n = RR_{n+1}$.

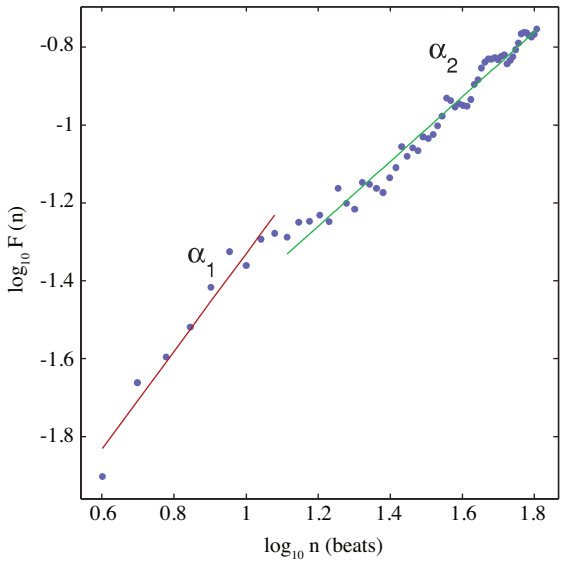

Figure 3. Detrended fluctuation analysis. A 2-sided logarithmic plot of index F(n) as a function of the segment length n, where α_1 and α_2 represent the short- and long-term variation slopes, respectively.

2.4. Feature selection

This study uses the automatic feature selection mechanism that selects better combinations from a variety of HRV parameters based on the CMs. After obtaining all of the HRV feature parameters involving time, frequency (FFT and AR), and nonlinear analysis, the following steps are followed:

- Calculate the CC value of every single feature parameter regarding the target column.
- Weigh the features as they correlate to the target and establish a weighting scale.
- Compute the mean value for each group.
- Sort the input scores in descending order.
- Select the parameters having CCs that are larger than the mean value of each group, regardless of their polarity.
- Carry the selected parameters as inputs to the NN classifiers.

2.5. The structure of the NN

As a classifier model, well-known FBPNNs with one hidden layer are utilized. Supervised training is applied to the datasets, which are equally divided into training and test groups. Overall, the classification accuracy is considered as the ratio of the correct decisions score to the number of total cases. The number of nodes of the input layer for all of the feature extraction methods is the same as the number of selected features. In the same way, the number of nodes of the output layer is the same as number of target classes. Each hidden layer has the average number of the nodes of the input and output layer. Figure 4 shows an example.

The optimal node number of hidden layers is found according to the total mean-squared error (MSE) values of the NNs at the same iteration. Figure 5 shows the MSE values of a 9-input, 2-output NN with a different number of nodes utilized in the hidden layer as an example.

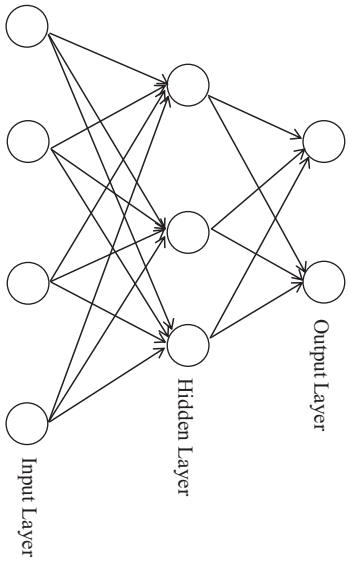

Figure 4. Three-layer feedforward network: input, hidden, and output layers, and nodes with feed forward links.

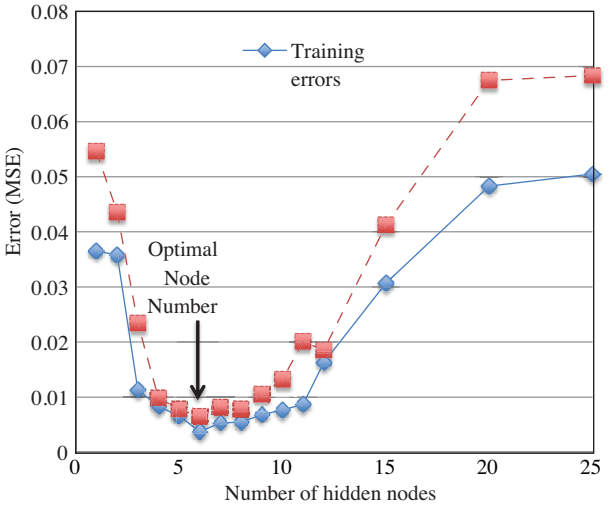

Figure 5. Selection of the optimum network architecture (i.e. the optimal node number of hidden layers is 6 for the 9-input, 2-output NN; the iteration number is kept constant at 500 for this analysis).

This experimentally decided optimal approach introduces a higher level of objectivity while comparing the relations between input features and output classes, and also keeps the same structure of the NNs utilized for different classification processes. Table 2 includes the input, hidden, and output layer sizes of the NNs of the applied methods.

Table 2. The number of nodes in the input, hidden, and output layers used in the FBPNNs.

Feature sets	Number of nodes		
	Input layer	Hidden layer	Output layer*
1. Only highly correlated (OHC) temporal parameters	5	4	2 or 3
2. OHC FFT spectral parameters	5	4	2 or 3
3. OHC AR spectral parameters	6	4	2 or 3
4. OHC nonlinear parameters	6	4	2 or 3
5. All parameters, including from 1 to 4	21	12	2 or 3
6. The parameters selected as OHC from 1 to 4	9	6	2 or 3

*: In the classification of 'apnea' and 'healthy' only, the number of output layers is 2. In the classification of 'apnea', 'hypopnea', and 'healthy', the number of output layers is 3.

The hyperbolic tangent sigmoid (tansig) transfer function is used for NNs. According to one study [36], the hyperbolic tangent function performs better recognition accuracy than those of the other transfer functions. This has been tested on MLPANNs, having the same iteration numbers and the same number of neurons in the hidden layer, with 5 different activation functions. Eq. (1) gives its function, and Figure 6 gives its graphical definitions.

$$\tan sig\,(n) = \frac{2}{1+e^{-2n}} - 1 \tag{1}$$

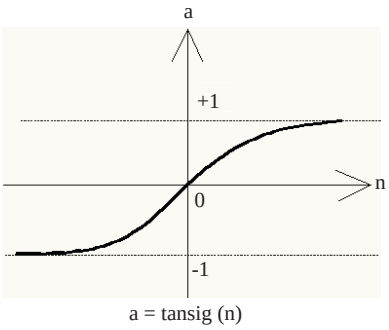

Figure 6. Transfer function graph.

2.6. Results

In this study, a high variety of HRV features are considered. In order to recognize the normal and disease conditions, the feature selection process is utilized on the classifier parameters. CMs are created with the parameters obtained from the temporal, frequency, and nonlinear parameters of the HRV presented in the tables. Table 3 gives the CMs of the TD HRV parameters used in the study.

In Table 2, pNN50, which defines 34% accuracy of the differentiation by this parameter alone, is the most important feature in the TD analysis. The mean HR is the negative maximum. The mean value of the temporal parameters is 0.177047, nearly half of the maximum value. Normally, the SD parameters' CCs (SDRR, SDHR,

SDANN, and SDNN index) are close to each other. Geometric feature parameters are not effective relative to the statistical features.

Table 3. CMs of the temporal parameters: n, negative; m, maximum; s, selected.

Feature parameters		|CC|
Statistical features	Mean RR (ms)	0.027201
	SDRR (ms)	0.168413 n
	Mean HR (1/min)	0.281809 ns
	SDHR (1/min)	0.122758
	RMSSD (ms)	0.27504 s
	NN50 (count)	0.294915 s
	pNN50 (%)	0.340003 sm
	SDANN (ms)	0.150295 n
	SDNN index (ms)	0.180253 ns
Geometric features	RR tri-index	0.09836 n
	TINN (ms)	0.008467
Mean value		0.177047

Table 4 gives the CMs of the FD of the HRV parameters for the HRV used in the study.

In Table 4, the HF relative power is the most important feature in the FFT and LF(n.u.) for the AR. LF(n.u.) for the FFT is also a negative maximum. The mean value of the FFT spectral parameters is 0.383521 and that of the AR spectral parameters is 0.304112. The normalized values of the LF and HF are the same without polarity. The absolute powers are less effective with respect to the relative and normalized power values. The peak frequency features are seen to be very different in FFT and AR.

Table 4. CMs of the FD parameters: n, negative; m, maximum; s, selected.

		FFT spectrum	AR spectrum
Feature parameters		|CC|	|CC|
Peak frequencies (Hz)	VLF	0	0. 199681
	LF	0.534047 s	2.02E-16 n
	HF	0.331492	0.020281 n
Absolute powers (ms^2)	VLF	0.172912 n	0.157111 n
	LF	0.008382 n	0.009564 n
	HF	0.378759	0.403538 s
Relative powers (%)	VLF	0.455515 ns	0.457622 ns
	LF	0.273168	0.260027
	HF	0.588302 sm	0.5954 s
Normalized powers	LF (n.u.)	0.557415 ns	0.600216 nsm
	HF (n.u.)	0.557415 s	0.600216 s
	LF/HF	0.361319	0.345686 ns
Mean value		0.383521	0.304112

Table 5 gives the CMs of the FD parameters for the HRV used in the study.

In Table 5, alpha 2 is observed to be the most valuable feature within the nonlinear features. The mean value is 0.387179, which is very close to the FFT mean. The entropy parameters (ShanEn, ApEn, and SampEn) are high and close to each other. Interestingly, the Poincaré plot parameters are not effective with respect to the other nonlinear parameters.

In Tables 3–5, each parameter has a CC value that describes a predictability of the classification numerically; the parameters with predictivities less than the mean CC values are eliminated, and from those having equal CC values, only one is taken and the polarity of the correlation is not considered. In Tables 3–5, the negative, maximum, and selected parameters' CC values are denoted by n, m, and s, respectively. Tables 2–4 show that the mean values of the nonlinear and FD features are almost the same and twice as high with respect to the temporal features. This rule also applies to the maximum values.

Figure 7A shows the classification and 7B shows the iteration results.

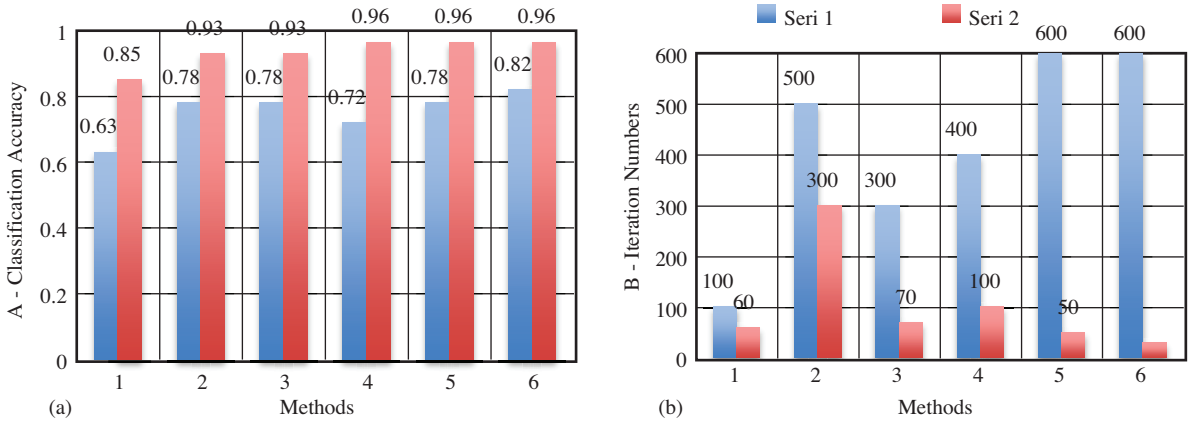

Figure 7. A) Classification and B) iteration results. Classes: A, apnea; B, hypopnea; C, healthy. Series: 1) results for 2 classes, A+B and C; 2) results for 3 classes: A, B, and C. Methods: 1) only highly correlated temporal parameters; 2) only highly correlated FFT spectral parameters; 3) only highly correlated AR spectral parameters; 4) only highly correlated nonlinear parameters; 5) all parameters including those from methods 1 to 4; 6) the parameters selected as only highly correlated from methods 1 to 4.

Table 5. CMs of the nonlinear parameters: n, negative; m, maximum; s, selected.

Feature parameters		|CC|
Poincaré plot	SD1 (ms)	0.275041
	SD2 (ms)	0.173002 n
RPA	Mean line length (beats)	0.174557 n
	Max line length (beats)	0.569607 ns
	REC (%)	0.159749 n
	DET (%)	0.586488 ns
	ShanEn	0.367369 n
DFA	alpha 1	0.556607 ns
	alpha 2	0.634889 nsm
Others	ApEn	0.441549 s
	SampEn	0.453813 s
	CD	0.253476
Mean value		0.387179

It can be seen from Figure 7A that the accuracy is ranked from high to low using the parameters of nonlinear, frequency, and TD, respectively. The accuracy is 96% for the classification of A and C (A: apnea, C: healthy) and 82% for the classification of A, B, and C (A: apnea, B: hypopnea, C: healthy), respectively.

An unexpected low accuracy is observed for the classification of A, B, and C using method 4. The other methods correlate to the input parameters' effectiveness, which are seen in Tables 3–5. Methods 4, 5, and 6

produced the same accuracy for the classification of A and C. However, the iterations are nearly twice as high. The iteration numbers are very high for the classification of A, B, and C (see Figure 7B).

3. Discussion and conclusions

The presented study offers a feature selection method to optimize classifier performance by means of realizing the classification task more accurately in a shorter time. The analysis is realized on a variety of features obtained from the time, spectral, and nonlinear components of heartbeat intervals. The results related to the performed accuracies with the dimension reduction on the feature sets clearly show that the CMs can be focused on reducing the feature sets and discarding the insignificant or less important features, along with being used for any type of diagnosis by numerically determining what features better represent the targeted disorder.

As a similar study in many aspects, Güneş et al. [37] proposed a new feature selection method called multiclass f-score feature selection combined with a multilayer perceptron artificial NN (MLPANN) in the classification of OSA. They used the clinical features obtained from a PSG device as a diagnostic tool for OSA in patients clinically suspected of suffering from this disease in order to determine the features related to OSA. These clinical features were the arousal index, AHI, SaO_2 minimum value in a stage of rapid eye movement, and the percent sleep time in a stage of SaO_2 intervals larger than 90%. The study selected the same features as in our study, and only the features that were bigger than the mean value were used in the classification. While the MLPANN obtained 63.41% classification accuracy in the diagnosis of OSA, the combination of the MLPANN and multiclass f-score feature selection achieved 84.14%.

Two studies [38,39] presented another example of an automated diagnostic system to feature selection combined with a NN to improve classifier accuracy. This diagnostic system consisted of a combined fuzzy clustering NN algorithm. The results demonstrated that the proposed diagnostic systems achieved a high (99%) accuracy rate.

Based on the results of this study, and looking at the other studies that used the same

Apnea-ECG database, the following can be concluded:

Six studies [40–45] made use of a spectral analysis of HRV. Two studies [40,46] employed the Hilbert transform to obtain spectral information of the HR. Three algorithms [40–42] used time-frequency maps of the HRV. In all of the FD techniques, the spectral power in the 0.01–0.04 Hz range was identified as an important parameter. Algorithms using a FD analysis received better results than those using a TD analysis, as in the present study. However, there were also some successful methods based on TD parameters. One approach utilized the time measurements of HRV with some nonlinear parameters [47] and the other TD method used rules implemented by a human administration for defining the periodic variation of the HR [48] to improve their results.

In some studies, several ECG-derived parameters different from HRV parameters were also used to diagnose, such as ECG pulse energy [41], R-wave duration [45], amplitude value of the S wave of each QRS [41], and ECG-derived respiration. The selected FD parameters with the R-wave morphology gave better results.

Acknowledgments

We would like to express gratitude to the Scientific and Technological Research Council of Turkey (TÜBİTAK). Hüseyin Gürüler was awarded a grant by TÜBİTAK. The grant number, name, and season are 2214-International Research Fellowship Program 2009/2.

References

[1] O. Sayadi, M.B. Shamsollahi, G.D. Clifford, "Synthetic ECG generation and Bayesian filtering using a Gaussian wave-based dynamical model", Physiological Measurement, Vol. 31, pp. 1309–1329, 2010.

[2] S.M.K. Jos, A.E. Spaan, Advances in Cardiac Signal Processing, Berlin, Springer-Verlag, 2007.

[3] H. Abdullah, N.C. Maddage, I. Cosic, D. Cvetkovic, "Cross-correlation of EEG frequency bands and heart rate variability for sleep apnoea classification", Medical & Biological Engineering & Computing, Vol. 48, pp. 1261–1269, 2010.

[4] M.J. Lado, X.A. Vila, L. Rodriguez-Linares, A.J. Mendez, D.N. Olivieri, P. Felix, "Detecting sleep apnea by heart rate variability analysis: assessing the validity of databases and algorithms", Journal of Medical Systems, Vol. 4, pp. 473–481, 2009.

[5] F. Roche, S. Celle, V. Pichot, J.C. Barthélémy, E. Sforza, "Analysis of the interbeat interval increment to detect obstructive sleep apnoea/hypopnoea", European Respiratory Journal, Vol. 29, pp. 1206–1211, 2007.

[6] B. Yilmaz, M.H. Asyali, E. Arikan, S. Yetkin, F. Ozgen, "Sleep stage and obstructive apneaic epoch classification using single-lead ECG", Biomedical Engineering Online, Vol. 9, pp. 39, 2010.

[7] P. de Chazal, C. Heneghan, E. Sheridan, R. Reilly, P. Nolan, M. O'Malley, "Automated processing of the single-lead electrocardiogram for the detection of obstructive sleep apnoea", IEEE Transactions on Biomedical Engineering, Vol. 50, pp. 686–696, 2003.

[8] C. O'Brien, C. Heneghan, "A comparison of algorithms for estimation of a respiratory signal from the surface electrocardiogram", Computers in Biology and Medicine, Vol. 37, pp. 305–314, 2007.

[9] M.O. Mendez, D.D. Ruini, O.P. Villantieri, M. Matteucci, T. Penzel, S. Cerutti, A.M. Bianchi, "Detection of sleep apnea from surface ECG based on features extracted by an autoregressive model", Conference Proceedings of the IEEE Engineering in Medicine and Biology Society, Vol. 2007, pp. 6106–6109, 2007.

[10] E. Sforza, S. Grandin, C. Jouny, T. Rochat, V. Ibanez, "Is waking electroencephalographic activity a predictor of daytime sleepiness in sleep-related breathing disorders?", European Respiratory Journal, Vol. 19, pp. 645–652, 2002.

[11] D. Alvarez, R. Hornero, J.V. Marcos, F. del Campo, "Multivariate analysis of blood oxygen saturation recordings in obstructive sleep apnea diagnosis", IEEE Transactions on Biomedical Engineering, Vol. 57, pp. 2816–2824, 2010.

[12] E. Goldshtein, A. Tarasiuk, Y. Zigel, "Automatic detection of obstructive sleep apnea using speech signals", IEEE Transactions on Biomedical Engineering, Vol. 58, pp. 1373–1382, 2011.

[13] T. Penzel, J. McNames, A. Murray, P. de Chazal, G. Moody, B. Raymond, "Systematic comparison of different algorithms for apnoea detection based on electrocardiogram recordings", Medical & Biological Engineering & Computing, Vol. 40, pp. 402–407, 2002.

[14] M.F. Hilton, R.A. Bates, K.R. Godfrey, M.J. Chappell, R.M. Cayton, "Evaluation of frequency and time-frequency spectral analysis of heart rate variability as a diagnostic marker of the sleep apnoea syndrome", Medical & Biological Engineering & Computing, Vol. 37, pp. 760–769, 1999.

[15] F. Roche, J.M. Gaspoz, I. Court-Fortune, P. Minini, V. Pichot, D. Duverney, F. Costes, J.R. Lacour, J.C. Barthelemy, "Screening of obstructive sleep apnea syndrome by heart rate variability analysis", Circulation, Vol. 100, pp. 1411–1415, 1999.

[16] J. Corthout, S. Van Huffel, M.O. Mendez, A.M. Bianchi, T. Penzel, S. Cerutti, "Automatic screening of obstructive sleep apnea from the ECG based on empirical mode decomposition and wavelet analysis", Proceedings of the 30th Annual International Conference of the IEEE Engineering in Medicine and Biology Society, Vol. 2008, pp. 3608–3611, 2008.

[17] M.O. Mendez, J. Corthout, S. Van Huffel, M. Matteucci, T. Penzel, S. Cerutti, A.M. Bianchi, "Automatic screening of obstructive sleep apnea from the ECG based on empirical mode decomposition and wavelet analysis", Physiological Measurement, Vol. 31, pp. 273–289, 2010.

[18] U.R. Acharya, K.P. Joseph, N. Kannathal, C.M. Lim, J.S. Suri, "Heart rate variability: a review", Medical and Biological Engineering and Computing, Vol. 44, pp. 1031–1051, 2006.

[19] A.F. Quiceno-Manrique, J.B. Alonso-Hernandez, C.M. Travieso-Gonzalez, M. A. Ferrer-Ballester, G. Castellanos-Dominguez, "Detection of obstructive sleep apnea in ECG recordings using time-frequency distributions and dynamic features", Conference Proceedings of the IEEE Engineering in Medicine and Biology Society, Vol. 2009, pp. 5559–5562, 2009.

[20] M.A. Al-Abed, M. Manry, J.R. Burk, E.A. Lucas, K. Behbehani, "Sleep disordered breathing detection using heart rate variability and R-peak envelope spectrogram", Conference Proceedings of the IEEE Engineering in Medicine and Biology Society, Vol. 2009, pp. 7106–7109, 2009.

[21] G.B. Moody, R.G. Mark, A.L. Goldberger, T. Penzel, "Stimulating rapid research advances via focused competition: the computers in cardiology challenge 2000", Computers in Cardiology 2000, pp. 207–210, 2000.

[22] T. Penzel, G.B. Moody, R.G. Mark, A.L. Goldberger, J.H. Peter, "Apnea-ECG database", Computers in Cardiology 2000, Vol. 27, pp. 255–258, 2000.

[23] W.R. Ruehland, P.D. Rochford, F.J. O'Donoghue, R.J. Pierce, P. Singh, A.T. Thornton, "The new AASM criteria for scoring hypopneas: impact on the apnea hypopnea index", Sleep, Vol. 32, pp. 150–157, 2009.

[24] J.P. Niskanen, M.P. Tarvainen, P.O. Ranta-Aho, P.A. Karjalainen, "Software for advanced HRV analysis", Computer Methods and Programs in Biomedicine, Vol. 76, pp. 73–81, 2004.

[25] A.J. Camm, M. Malik, J.T. Bigger, G. Breithardt, S. Cerutti, R.J. Cohen, P. Coumel, E.L. Fallen, H.L. Kennedy, R.E. Kleiger, F. Lombardi, A. Malliani, A.J. Moss, J.N. Rottman, G. Schmidt, P.J. Schwartz, D.H. Singer, "Heart rate variability: standards of measurement, physiological interpretation and clinical use. Task Force of the European Society of Cardiology and the North American Society of Pacing and Electrophysiology", Circulation, Vol. 93, pp. 1043–1065, 1996.

[26] M. Brennan, M. Palaniswami, P. Kamen, "Do existing measures of Poincare plot geometry reflect nonlinear features of heart rate variability?", IEEE Transactions on Biomedical Engineering, Vol. 48, pp. 1342–1347, 2001.

[27] S. Carrasco, M.J. Gaitan, R. Gonzalez, O. Yanez, "Correlation among Poincare plot indexes and time and frequency domain measures of heart rate variability", Journal of Medical Engineering and Technology, Vol. 25, pp. 240–248, 2001.

[28] J.S. Richman, J.R. Moorman, "Physiological time-series analysis using approximate entropy and sample entropy", American Journal of Physiology-Heart and Circulatory Physiology, Vol. 278, pp. 2039–2049, 2000.

[29] H.B.Y. Fusheng, T. Qingyu, "Approximate entropy and its application in biosignal analysis", in M. Akay, editor, Nonlinear Biomedical Signal Processing: Dynamic Analysis and Modeling, Vol. 2, New York, IEEE Press, pp. 72–91, 2001.

[30] C.K. Peng, S. Havlin, H.E. Stanley, A.L. Goldberger, "Quantification of scaling exponents and crossover phenomena in nonstationary heartbeat time-series", Chaos, Vol. 5, pp. 82–87, 1995.

[31] S. Guzzetti, M.G. Signorini, C. Cogliati, S. Mezzetti, A. Porta, S. Cerutti, A. Malliani, "Non-linear dynamics and chaotic indices in heart rate variability of normal subjects and heart-transplanted patients", Cardiovascular Research, Vol. 31, pp. 441–446, 1996.

[32] C.L. Webber, J.P. Zbilut, "Dynamical assessment of physiological systems and states using recurrence plot strategies", Journal of Applied Physiology, Vol. 76, pp. 965–973, 1994.

[33] D.E. Lake, J.S. Richman, M.P. Griffin, J.R. Moorman, "Sample entropy analysis of neonatal heart rate variability", American Journal of Physiology-Regulatory Integrative and Comparative Physiology, Vol. 283, pp. R789–R797, 2002.

[34] T. Penzel, J.W. Kantelhardt, L. Grote, J.H. Peter, A. Bunde, "Comparison of detrended fluctuation analysis and spectral analysis for heart rate variability in sleep and sleep apnea", IEEE Transactions on Biomedical Engineering, Vol. 50, pp. 1143–1151, 2003.

[35] P. Grassberger, I. Procaccia, "Characterization of strange attractors", Physical Review Letters, Vol. 50, pp. 346–349, 1983.

[36] B. Karlik, A.V. Olgaç, "Performance analysis of various activation functions in generalized MLP architectures of neural networks", International Journal of Artificial Intelligence and Expert Systems, Vol. 1, pp. 111–122, 2011.

[37] S. Güneş, K. Polat, Ş. Yosunkaya, "Multi-class f-score feature selection approach to classification of obstructive sleep apnea syndrome", Expert Systems with Applications, Vol. 37, pp. 998–1004, 2010.

[38] Y. Özbay, R. Ceylan, B. Karlik, "A fuzzy clustering neural network architecture for classification of ECG arrhythmias", Computers in Biology and Medicine, Vol. 36, pp. 376–388, 2006.

[39] R. Ceylan, Y. Özbay, B. Karlik, "A novel approach for classification of ECG arrhythmias: type-2 fuzzy clustering neural network", Expert Systems with Applications, Vol. 36, pp. 6721–6726, 2009.

[40] M. Schrader, C. Zywietz, V. von Einem, B. Widiger, G. Joseph, "Detection of sleep apnea in single channel ECGs from the Physionet data base", Computers in Cardiology 2000, Vol. 27, pp. 263–266, 2000.

[41] J.N. McNames, A.M. Fraser, "Obstructive sleep apnea classification based on spectrogram patterns in the electrocardiogram", Computers in Cardiology 2000, Vol. 27, pp. 749–752, 2000.

[42] M.R. Jarvis, P.P. Mitra, "Apnea patients characterized by 0.02 Hz peak in the multitaper spectrogram of electrocardiogram signals", Computers in Cardiology 2000, Vol. 27, pp. 769–772, 2000.

[43] M.J. Drinnan, J. Allen, P. Langley, A. Murray, "Detection of sleep apnoea from frequency analysis of heart rate variability", Computers in Cardiology 2000, Vol. 27, pp. 259–262, 2000.

[44] P. de Chazal, C. Heneghan, E. Sheridan, R. Reilly, P. Nolan, M. O'Malley, "Automatic classification of sleep apnea epochs using the electrocardiogram", Computers in Cardiology 2000, Vol. 27, pp. 745–748, 2000.

[45] Z. Shinar, A. Baharav, S. Akselrod, "Obstructive sleep apnea detection based on electrocardiogram analysis", Computers in Cardiology 2000, Vol. 27, pp. 757–760, 2000.

[46] J.E. Mietus, C.K. Peng, P.C. Ivanov, A.L. Goldberger, "Detection of obstructive sleep apnea from cardiac interbeat interval time series", Computers in Cardiology 2000, Vol. 27, pp. 753–756, 2000.

[47] C. Maier, M. Bauch, H. Dickhaus, "Recognition and quantification of sleep apnea by analysis of heart rate variability parameters", Computers in Cardiology 2000, Vol. 27, pp. 741–744, 2000.

[48] P.K. Stein, P.P. Domitrovich, "Detecting OSAHS from patterns seen on heart-rate tachograms", Computers in Cardiology 2000, Vol. 27, pp. 271–274, 2000.

Appendix. Summary of the HRV measures.

Measures		Units	Description	Equation
Time-domain	$\overline{RR}$	(ms)	Mean of the RR intervals	
	SDNN	(ms)	SD of the RR intervals	$SDNN = \sqrt{\frac{1}{N-1}\sum_{j=1}^{N}\left(RR_j - \overline{RR}\right)^2}$
	$\overline{HR}$	(1/min)	Mean of the HR	
	SDHR	(1/min)	SD of instantaneous HR values	$SDHR = \sqrt{\frac{1}{N-1}\sum_{j=1}^{N}\left(HR_j - \overline{HR}\right)^2}$
	RMSSD	(ms)	Root mean square of the successive differences	$RMSSD = \sqrt{\frac{1}{N-1}\sum_{j=1}^{N-1}\left(RR_{j+1} - RR_j\right)^2}$
	NN50	Number of successive RR intervals that differ by more than 50 ms		
	pNN50	(%)	Percentage of NN50	$pNN50 = \frac{NN50}{N-1}\times 100\%$
	HRV triangular index	The integral of the density distribution for the RR interval histogram		
	TINN	(ms)	Baseline width of the RR interval histogram	
Frequency	Peak frequency	(Hz)	Peak frequencies of VLF, LF, and HF bands	
	Absolute power	(ms^2)	Absolute powers of the VLF, LF, and HF bands	
	Relative power	(%)	Relative powers of the VLF, LF, and HF bands	
	Normalized power	(n.u.)	LF and HF band powers in normalized units	
Nonlinear	SD1, SD2	(ms)	The SDs of the Poincaré plot, vertical SD1 and horizontal SD2	$SD1 = \frac{SDSD^*}{\sqrt{2}}$ $SD2 = \sqrt{2SDNN^2 - SD1^2}$ $*SDSD = \sqrt{E\{\Delta RR_j^2\} - E\{\Delta RR_j\}^2}$
	ApEn	Approximate entropy		$ApEn(m, r, N) = \Phi^m(r) - \Phi^{m+1}(r)$
	SampEn	Sample entropy		$SampEn(m, r, N) = \ln(C^m(r)/C^{m+1}(r))$
	D_2	Correlation dimension		$D_2(m) = \lim_{l\to 0}\lim_{N\to\infty}\frac{\log C^m(r)}{\log r}$
	DFA	Detrended fluctuation analysis		
	α_1 and α_2	Short- and long-term fluctuation slopes, respectively		
	RP	Recurrence plot analysis		$RP(j,k) = \begin{cases}1, & d(u_j - u_k) \le r\\ 0, & \text{otherwise}\end{cases}$
	Lmean	(beats)	Mean line length	$l_{mean} = \frac{\sum_{l=l_{min}}^{l_{max}} l\, N_l}{\sum_{l=l_{min}}^{l_{max}} N_l}$
	REC	(%)	Recurrence rate	$REC = \frac{1}{(N-m+1)}\sum_{j,k=1}^{N-m+1} RP(j,k)$
	DET	(%)	Determinism	$DET = \frac{\sum_{l=l_{min}}^{l_{max}} l\, N_l}{\sum_{j,k=1}^{N-m+1} RP(j,k)}$
	ShanEn		Shannon entropy	$ShanEn = -\sum_{l=l_{min}}^{l_{max}} n_l \ln n_l$